Research Square

Preprints are preliminary reports that have not undergone peer review.
They should not be considered conclusive, used to inform clinical practice,
or referenced by the media as validated information.

Microbiome dynamics in healthy and SCTLD diseased colonies of foundational coral species in La Parguera, Puerto Rico

Joyce Marie Gómez Samot
University of Puerto Rico-Mayaguez
Nikolaos V Schizas
nikolaos.schizas@upr.edu

University of Puerto Rico-Mayaguez
Alex J Veglia
University of Puerto Rico-Mayaguez
Juan J Cruz Motta
University of Puerto Rico-Mayaguez
Ernesto Weil
University of Puerto Rico-Mayaguez

Research Article

Keywords: scleractinian coral, coral microbiome, Caribbean, microbial dysbiosis, disease progression

Posted Date: June 15th, 2026

DOI: https://doi.org/10.21203/rs.3.rs-9430109/v1

License: This work is licensed under a Creative Commons Attribution 4.0 International License.
Read Full License

Additional Declarations: No competing interests reported.

Abstract

Stony Coral Tissue Loss Disease (SCTLD) is a rapidly spreading coral disease that has caused significant mortality throughout the northern Caribbean. Curiously, its underlying causes and microbiome dynamics remain unclear. In this study, the temporal dynamics of bacterial communities were characterized in five foundational coral species: *Montastraea cavernosa*, *Colpophyllia natans*, *Pseudodiploria strigosa*, *Diploria labyrinthiformis*, and *Orbicella faveolata* in La Parguera Natural Reserve (LPNR), southwest Puerto Rico. At least 10 healthy, tagged colonies from each species were sampled prior to SCTLD's arrival in LPNR and then resampled upon infection. Samples from the infected margin and the healthy-looking tissues of the same colonies, as well as from five nearby healthy controls of each species, were taken and frozen at -80ºC. Microbial communities were analyzed using 16S rRNA gene amplicon sequencing. Bacterial communities were dominated by Alphaproteobacteria, Gammaproteobacteria, and Bacteroidia across species and health conditions. Within species, PERMANOVA results showed significant differences in microbial composition between infected and healthy-looking tissues ($R^2 = 0.09–0.34$, $p < 0.05$), with variation across taxa. Differences were more pronounced in M. cavernosa and P. strigosa, whereas the overlap was greater in other species. Differential abundance analyses revealed enrichment of taxa associated with opportunistic and anaerobic processes in diseased tissues, including members of Clostridia (e.g., Tepidibacter) and sulfate-reducing bacteria, although these patterns were not consistent across all coral species. These results align with previous studies, showing shifts toward opportunistic and anaerobic microbial groups in SCTLD, while showing that these changes vary in structure and magnitude across coral hosts rather than being driven by a single causative bacterial pathogen.

Introduction

Coral reefs are biodiversity hotspots that host myriad species (Reaka-Kudla, 1997). Through continuous calcification, scleractinian corals form the foundation of these highly complex reef structures (van Oppen & Blackall, 2019). Beyond their ecological role, coral reefs also contribute to coastal protection, support fisheries, and provide important benefits to human communities that rely on them (Moberg & Folke, 1999; Ferrario et al., 2014). During the last decades however, coral reefs communities around the world have been showing significant deterioration mostly due to massive coral mortalities produced by frequent epizootic events of new and old diseases and increasing frequency and intensity of bleaching events associated with increasingly hot thermal anomalies (global warming) and aided by synergistic anthropogenic impacts (Harvell et. al., 2007, 2009; Hughes 1994, 2003; Hoegh-Guldberg et. al. 1997; Bruno et al. 2007; Weil et. al. 2009a,b; Weil and Rogers, 2011; Burge et. al. 2014; Jackson et al. 2014; Aronson et. a. 2016; McClanahan et. al. 2017; Weil et. al. 2017; 2019; Vega-Thurber et. al. 2020). The frequency of these events is hindering natural recovery by sexual reproduction and natural growth in most localities by minimizing favorable periods of time after disturbances, especially for the slow-growing, massive, reef-building species compared to those species with high growth rates and clonal expansion (Weil et. al.,2017; 2019; Tuohy et al., 2015; Jackson et al., 2014; Hughes et al., 2017).

At the scale of individual coral colonies, each colony functions as a holobiont, comprising the host and a diverse array of microorganisms including bacteria, archaea, algae, fungi, and viruses (Bourne et al., 2016; van Oppen & Blackall, 2019). Microbial community composition plays important roles in physiological functioning and stability and is hypothesized to influence coral susceptibility to disease and the severity of microbiome disruption during infection (Rosenberg et al., 2007; Zaneveld et al., 2016; Vega Thurber et al., 2025).

Stony Coral Tissue Loss Disease (SCTLD) is among the most destructive coral diseases documented to date (Precht et al., 2016; Aeby et al., 2019; Croquer et al., 2021). Emerging in 2014 after dredging the Port of Miami (Precht et al. 2016), it has rapidly spread throughout the Caribbean, affecting more than 20 coral species (Aeby et al., 2019; Wei et al., 2019; Landsberg et al., 2020). SCTLD is characterized by multifocal lesions, rapid tissue loss, and high mortality. It has also been associated with disruptions to the coral-algal symbiosis and breakdown of the coral holobiont, although its exact cause remains unknown (Landsberg et al., 2020; Rossin et al., 2026). The impact of infection varies across coral species and among individuals within the same species, demonstrated by previously reported differences in lesion disease prevalence, progression, and severity (Aeby et al., 2019; Landsberg et al., 2020; Meyer et al., 2019; Weil et. al., 2019).

Although bacterial groups such as *Vibrio* and members of Rhodobacterales, Rhizobiales, and Clostridia have been detected in SCTLD lesions, no single pathogen has been consistently identified, suggesting that the disease is not driven by a single causative agent but rather by complex microbial interactions (Meyer et al., 2019; Rosales et al., 2020; Ushijima et al., 2020; Arriaga-Piñón et al., 2021). Recent studies indicate that these taxa are commonly enriched in diseased corals but may also be present in apparently healthy corals, surrounding seawater, and sediments in affected reef systems, highlighting their potential role in disease dynamics rather than as primary pathogens (Vega-Thurber et al, 2020; Rosales et al., 2020; Clark et al., 2021; Nandi et al., 2022).

In this context, SCTLD is increasingly viewed as a disease characterized by shifts in microbial community structure associated with stress and dysbiosis, in which microbial changes may reflect and contribute to disease progression rather than act as direct causes (Peixoto et al., 2017; Zaneveld et al., 2016).

In Puerto Rico, SCTLD was first reported on reefs in 2019 off the east coast and has since spread across shallow and deep reef systems (Weil et al., 2019; Lucas et al., 2024; Williams et al., 2021). The reefs of La Parguera Natural Reserve (LPNR) have been subjected to long-term monitoring at several nearshore and offshore sites before, during, and after the SCTLD epizootic. Existing baseline information provides a unique opportunity to investigate the temporal dynamics of the coral microbiome in healthy and SCTLD-infected colonies across different species in Puerto Rico. Characterizing and comparing the impact of infection on coral microbiomes across time and geographic locations will reveal shared patterns, shedding light on the potential role of bacteria in disease development and, perhaps, the putative causes of the diseases.

This study examined how coral-associated bacterial communities change in response to Stony Coral Tissue Loss Disease across multiple host species in the LPNR. Specifically, we asked whether (1) microbial communities differ among tissue conditions within colonies, including apparently healthy tissue (HH), visually unaffected tissue within diseased colonies (HD), and lesion margins (DD), and (2) microbiome shifts associated with disease are consistent across species or exhibit host-specific patterns.

We hypothesized that microbial community composition would differ significantly across tissue conditions, with DD samples showing the greatest divergence from HH samples, and that HD samples would exhibit intermediate or transitional community states. Additionally, we expected that the magnitude and nature of these shifts would vary among coral species, reflecting host-specific responses to infection rather than a single, uniform microbial signature of disease.

Materials and Methods

Sample collection

Fieldwork was conducted within La Parguera Natural Reserve (LPNR) on the southwest coast of Puerto Rico, a region containing some of the island's most developed and highly diverse coral reefs. At least 10 healthy-looking colonies of each of five foundational coral species; *Montastraea cavernosa* (n = 23), *Colpophyllia natans* (n = 35), *Pseudodiploria strigosa* (n = 25), *Diploria labyrinthiformis* (n = 17), and *Orbicella faveolata* (n = 32), were tagged in three reef localities: Turrumote (17º 56.097N − 67º 01.130W) a mid-shelf fringing reef; San Cristobal (17˚ 56.298N − 67˚ 04.298W) a mid-shelf patch reef, and Buoy (17˚ 53.291 ' N -66° 59.884W). All were located near the marine lab of the Department of Marine Sciences at Isla Magueyes (Fig. 1). Tagged colonies were located along or near established permanent transects, making them easy to find and monitor over time.

Before SCTLD was detected in the area, three replicate samples were collected from at least 15 visually healthy tagged colonies of each species (HH) by scraping and suctioning tissue/mucus/skeleton from the surface tissue with labeled, needleless sterile 50ml syringes. Syringes from the same colony were placed in Whirlpack bags and brought to the boat where they were placed on ice in a cooler, transported to the lab and dump into the − 80ºC ultra-freezer for later processing.

After SCTLD got to LPRN and infected most tagged colonies, two replicate samples were collected the same way from active diseased lesion margin (DD) and two from apparently healthy tissue within the same colony (HD) of each of at least 10 tagged colonies of each species.

At the time diseased samples were collected, two replicate samples of at least three nearby visually healthy corals of the same species were also sampled as controls (CC). All samples were placed in a cooler with ice and transported to the lab, where they were stored in a -80°C ultra-freezer for later processing. Replicates were collected from spatially separated areas within each colony to account for within-host variability.

All sampling and related field activities were conducted under permit #2020-IC-017 – O-VS-PVS15-SJ-01097-05112019 from the Department of Natural and Environmental Resources of Puerto Rico.

DNA analyses were conducted separately for each species to account for differences in baseline microbial communities and species-specific responses to SCTLD. The final dataset used for downstream analyses comprised 133 samples across five coral species and four health states (Table 1). Sampling effort varied among species due to differences in sample yield and tissue availability during collection and processing.

Table 1
Number of colonies and tissue samples collected across coral species and health states. Health conditions are defined as follows: HH = apparently healthy colonies sampled prior to SCTLD detection in La Parguera Natural Reserve; DD = lesion margin tissue from diseased colonies; HD = apparently healthy tissue within diseased colonies; CC = visually healthy control colonies sampled at the same time and sites as diseased colonies.

Species	Total colonies	HH	DD	HD	CC	Total tissue samples
C. natans	8	11	11	13	4	39
D. labyrinthiformis	6	9	5	10	5	29
M. cavernosa	6	5	9	8	7	29
O. faveolata	3	3	2	3	4	12
P. strigosa	4	6	5	7	6	24
Total (n)	27	34	32	41	26	133

Sample processing and amplification

All genomic DNA extractions were done using the DNeasy PowerSoil Pro Kit (QIAGEN, Germantown, MD), with minor modifications to the manufacturer's protocol. Prior to extraction, syringe contents were thawed at room temperature (25°C) and transferred to 50 mL centrifuge tubes while still cold. Samples were centrifuged at 3,000 rpm (~ 1,150 × g) for 15 minutes to concentrate particulate material. The resulting pellet was resuspended in 600 µL of CD1 solution. Subsequently, 200 µL of the resuspended material was transferred into each of three PowerBead Pro tubes, each preloaded with 600 µL of CD1, resulting in a total volume of 800 µL CD1 per tube. Samples were then homogenized using a FastPrep FP120 instrument (Thermo Electron Corporation, USA) for 15 seconds at 4.0 m/s, with tubes placed on ice for one minute between three iterations. After homogenization, the tubes were placed on ice for an additional 2 minutes, then centrifuged. The remaining steps followed the standard PowerSoil Pro Kit protocol.

DNA quality and quantity were assessed using a Qubit 4 Fluorometer and 1% agarose gel electrophoresis. The V4 region of the bacterial 16S rRNA gene was amplified using primers 515F

(GTGCCAGCMGCCGCGGTAA; original Earth Microbiome Project; Parada et al., 2016) and 806R (GGACTACVSGGGTATCTAAT; Apprill et al., 2015) by Admera Health Biopharma Services. PCR reactions contained 1 µL of template DNA and were run with the HotStarTaq Plus Kit under the following cycling conditions: 94°C for 3 min; 30 cycles of 94°C for 30 s, 53°C for 40 s, and 72°C for 1 min; followed by a final elongation at 72°C for 5 min (Clark et al., 2021). Resulting amplicons were sequenced on an Illumina MiSeq platform (2 × 250 bp paired-end reads) with a target of 100,000 reads per sample.

Bioinformatics and taxonomy assignment of Amplicon Sequence Variants (ASV)

All bioinformatics analyses were performed in QIIME 2 (version 2024.2) for sequence quality control, feature inference, and taxonomic classification (Bolyen et al., 2019). The amplified 16S rRNA V4 region (~ 250 bp) was used for downstream processing. Raw paired-end reads were delivered in FASTQ format and imported into QIIME 2 via a manifest-based workflow. After import, sequence quality was evaluated using the qiime demux summarize function to visualize per-base quality profiles and guide trimming parameter settings using the DADA2 algorithm (Callahan et al., 2016) implemented within QIIME 2.Sequence denoising and ASV processing were carried out using the qiime dada2 denoise-paired plugin. Forward and reverse reads were trimmed by 19 and 20 bp, respectively, to remove primer sequences, and truncated at 230 bp (forward) and 220 bp (reverse) based on quality score profiles. This step included merging reads and removing chimeras for high-resolution amplicon sequence variants (ASVs).

Following ASV identification, taxonomy was assigned using the pre-trained silva-138-99-515-806-nb-classifier. To standardize sequencing depth across samples for diversity analyses, the ASV table was rarefied to 10,000 reads per sample using the qiime feature-table rarefy command. This threshold was selected to retain most samples while minimizing bias arising from uneven sequencing depth. All resulting artifacts, including the feature table, taxonomy assignments, and rooted phylogenetic tree, were exported for downstream statistical analyses and visualization in RStudio.

Community Diversity Analyses

All statistical analyses were conducted in R version 4.3.2 (R Core Team, 2023) using RStudio (version 2026.01.1), with the packages *phyloseq*, *vegan*, *ggplot2*, and *dplyr*. The ASV table, taxonomy table, phylogenetic tree, and sample metadata were integrated into a single phyloseq object for downstream analyses.Prior to any analyses, sequences assigned to mitochondria, chloroplasts, and Eukaryota were removed from the dataset. Taxonomic annotations with missing classifications at lower ranks were labeled as “Unclassified” to maintain consistency across taxonomic levels. After removing these sequences, the dataset was inspected at the genus level for taxa commonly reported as potential contaminants in low-biomass microbiome studies. Although some genera of interest were detected, they were not consistently dominant across samples and were therefore retained for further analyses.

ASV counts were converted to relative abundances for compositional analyses to account for differences in sequencing depth among samples, while alpha diversity metrics were computed from rarefied data. Alpha diversity was quantified using the Shannon diversity index (H') to describe within-sample diversity across coral species and tissue conditions. Shannon values were calculated with the estimate_richness() function in phyloseq and visualized with ggplot2 as boxplots with overlaid sample points. Differences in alpha diversity among tissue conditions were tested separately for each species using Kruskal-Wallis tests (implemented in R with the kruskal.test() function) (Table S1). When significant, pairwise Wilcoxon rank-sum tests were performed using pairwise.wilcox.test() function, and p-values were adjusted for multiple comparisons using the Benjamini-Hochberg method (Table S2).

Taxonomic composition and relative abundance patterns were summarized at multiple taxonomic levels by agglomerating ASVs using the tax_glom() function (e.g., order, family, or genus). The resulting tables were visualized as stacked bar plots using ggplot2 to illustrate the relative contribution of dominant bacterial groups across species and tissue conditions.

To further examine changes in individual taxa associated with disease, differential abundance analyses were conducted at the genus level. Genera showing significant differences among tissue conditions were identified using Kruskal-Wallis tests, followed by pairwise Wilcoxon rank-sum tests with p-values adjusted for multiple comparisons. Heatmaps were constructed using a subset of taxa with the largest and most consistent differences across conditions. Because patterns of community differentiation varied across coral species, heatmaps were limited to three species that showed the clearest separation among tissue conditions, as indicated by beta-diversity and differential-abundance analyses. Mean relative abundances were calculated for each genus within each tissue condition and species, and values were log10(x + 1)-transformed prior to visualization. Heatmaps were generated using ggplot2.

Beta diversity was assessed using Bray-Curtis dissimilarity, computed with the vegdist() function in the vegan package (Jari Oksanen et al., 2022). Non-metric multidimensional scaling (NMDS) ordination was performed with the metaMDS() function to visualize differences in microbial community structure among coral species and health states. NMDS results were visualized with ggplot2, with points colored by species and/or health status, and ellipses were added to highlight clustering within groups.

Differences in community composition were tested using permutational multivariate analysis of variance (PERMANOVA) implemented with the adonis() function in vegan, using a model including coral species and health state as explanatory variables. The number of permutations was set to 999. Homogeneity of multivariate dispersion among groups was evaluated using betadisper() and permutest().

Results

Microbial community composition across coral species

Microbial community composition varied across coral species, with a consistent dominance of a few major bacterial groups. Members of the classes Alphaproteobacteria, Gammaproteobacteria, and

Bacteroidia represented most of the community across species and health states, although their relative abundances differed among species and health conditions (Fig. 1).

Species-specific patterns were evident. For example, *C. natans*, *D. labyrinthiformis*, and *O. faveolata* showed higher relative contributions of Gammaproteobacteria, while *Montastraea cavernosa* and *P. strigosa* had a more even distribution among major classes, with greater contributions from other groups such as Alphaproteobacteria and Bacteroidia. In contrast, *O. faveolata* was characterized by a higher relative contribution of Bacteroidia compared to the other species.

Differences associated with health state were also observed within species. Diseased tissues (DD) showed changes in relative abundance compared with healthy tissues (HH), mainly in some lower-abundance groups. Increases in Clostridia were observed in multiple species, particularly in *M. cavernosa*, *P. strigosa*, and *C. natans*, although this pattern was not consistent across all species. Members of Desulfovibrionia were also detected in some diseased samples, especially in *M. cavernosa*, but were also present at lower abundances in other health states.

Overall, these patterns indicate that changes in microbial composition during disease are variable across species, supporting species-specific microbiome responses to SCTLD.

Microbial communities driven by species, then health state

NMDS analyses were performed separately for each species to better resolve patterns associated with the health state. Non-metric multidimensional scaling (NMDS) based on Bray-Curtis dissimilarity revealed clear differences in microbial community structure among coral species (Fig. 2). Within species, separation by health state was variable. In *M. cavernosa* and *P. strigosa*, diseased (DD) and healthy (HH) samples showed partial separation, suggesting shifts in microbial community structure associated with SCTLD. In contrast, other species showed greater overlap between health states, indicating more subtle or variable microbiome responses.

PERMANOVA confirmed that both species and health state contributed to differences in community composition, although the strength of these effects varied among species (Table S3). The proportion of variance explained by health state ranged from 0.09 in *C. natans* ($R^2 = 0.094$, $p = 0.011$) to 0.34 in *O. faveolata* ($R^2 = 0.336$, $p = 0.006$). Intermediate effects were observed in *M. cavernosa* ($R^2 = 0.161$, $p = 0.002$), *P. strigosa* ($R^2 = 0.164$, $p = 0.001$), and *D. labyrinthiformis* ($R^2 = 0.128$, $p = 0.017$).

Homogeneity of dispersion tests varied among species, with significant differences observed in *C. natans* and *D. labyrinthiformis* ($p < 0.05$), whereas other species showed no significant differences. This suggests that PERMANOVA results should be interpreted with caution, as some differences may be driven by variation in dispersion.

Differentially abundant taxa across health states

Differential abundance analyses revealed multiple taxa that differed significantly between healthy (HH) and diseased (DD) tissues, although these patterns varied among coral species (Fig. 3). Across species, diseased tissues were often associated with increases in several less abundant taxa, including groups commonly linked to opportunistic or anaerobic processes (e.g., Clostridiales and Desulfovibrionales), although these trends were not consistent across all hosts. In contrast, healthy tissues tended to be associated with taxa that were more consistently present across samples.

The magnitude and direction of these shifts differed among species (Fig. 3); more pronounced differences between HH and DD states were observed in *M. cavernosa* and *P. strigosa*, and more moderate changes in *C. natans*. Genus-level variation among tissue conditions was assessed using Kruskal-Wallis tests with post-hoc pairwise comparisons, identifying multiple taxa with significant variation across health states ($p < 0.05$; Table S4). These included genera such as *Tepidibacter*, *Fusibacter*, and *Marinifilum*, as well as sulfate-reducing groups such as *Halodesulfovibrio*. Heatmap visualizations (Fig. 3) focus on species with more pronounced shifts among tissue conditions ($R^2 \geq$ ~0.15, based on PERMANOVA) to improve clarity, while full results across all taxa and species are provided in Table S4.

Alpha diversity patterns across species and health states

Alpha diversity, measured using the Shannon index, varied across species and health states (Fig. 5). *C. natans* showed slightly higher diversity in DD compared to HH, whereas *M. cavernosa* and *D. labyrinthiformis* showed lower diversity in DD samples. In *P. strigosa* and *O. faveolata*, differences among health states were less consistent.Kruskal-Wallis tests indicated that alpha diversity differed significantly among health states only in *M. cavernosa* ($p < 0.05$), whereas no significant differences were detected in the other species (Table S1). Pairwise comparisons further showed that Shannon diversity in DD samples differed significantly from HH, CC, and HD in *M. cavernosa* (adjusted $p < 0.05$; Table S2).

Discussion

This study examined how microbial communities associated with healthy and SCTLD-affected corals change across different health conditions in LPNR. Microbial communities were dominated by members of Alphaproteobacteria, Gammaproteobacteria, and Bacteroidia, consistent with patterns reported in other Caribbean reefs (Meyer et al., 2019; Rosales et al., 2020). Differences in relative abundance among these major groups varied across species and health conditions, indicating that baseline microbiome composition is host-dependent and may influence how communities respond to disease. Across conditions, diseased tissues were often associated with increases in less abundant taxa, particularly groups linked to anaerobic metabolism and tissue degradation (Fig. 2).

NMDS and PERMANOVA results showed that health status significantly affected microbial community composition, although the strength of this effect varied among hosts, with PERMANOVA R^2 values ranging from 0.09 in *C. natans* to 0.34 in *O. faveolata* (Table S3, Fig. 3). A clearer separation between

healthy and diseased samples was observed in *M. cavernosa* and *P. strigosa*, while other species showed more overlap, suggesting that some corals undergo more noticeable microbiome shifts during SCTLD. Comparable patterns have been observed in experimental studies, in which microbiome responses to SCTLD vary across coral species (Huntley et al., 2022). Differences in dispersion were observed in some species (e.g., *C. natans* and *D. labyrinthiformis*), indicating that part of the variation detected by PERMANOVA may reflect within-group variability, in addition to shifts in community composition (Table S3, Fig. 3).

Differential abundance analyses further confirm these patterns. Diseased tissues exhibited increases in several taxa, including members of Clostridia (e.g., Peptostreptococcaceae and *Tepidibacter*) and Desulfovibrionia (e.g., *Halodesulfovibrio*), particularly in *M. cavernosa* and *C. natans* (Fig. 4). These groups are associated with anaerobic metabolism and tissue degradation and have been repeatedly reported in SCTLD-affected corals (Meyer et al., 2019; Rosales et al., 2020). In contrast, taxa such as members of the Rhodobacteraceae and Endozoicomonas, which are often associated with stable and healthy coral microbiomes (Ainsworth et al., 2015; Neave et al., 2016), were more frequently observed in healthy tissues (Fig. 4).

Alpha diversity patterns were also inconsistent across species. Some species showed increases in diversity in diseased tissues, while others showed decreases or little change (Fig. 5). Overall, there was no clear trend, suggesting that SCTLD is not associated with a consistent shift in diversity but rather with changes in community composition.

These patterns align with findings from other SCTLD microbiome studies across the Caribbean. In the Florida Reef Tract, Meyer et al. (2019) reported communities dominated by Alphaproteobacteria, Gammaproteobacteria, and Bacteroidia, with diseased tissues enriched in opportunistic taxa. Rosales et al. (2023) similarly identified recurrent enrichment of anaerobic and opportunistic groups, including Clostridia, Campylobacteria, and sulfate-reducing bacteria, along with declines in taxa commonly associated with healthy corals such as *Endozoicomonas*. The enrichment of Clostridia and Desulfovibrionia observed here supports these patterns (Fig. 2, Fig. 3). Because this study includes repeated sampling of the same colonies before and after disease onset, these patterns provide additional support that microbiome shifts are associated with disease progression rather than natural variation among colonies.

In the Mexican Caribbean, Arriaga-Piñón et al. (2024) reported shifts in microbial communities associated with SCTLD, including enrichment of genera such as *Vibrio*, *Photobacterium*, *Spirochaeta*, and *Nitrospira*. While not all these genera were dominant in our study, we observed increases in functionally similar groups, particularly anaerobic and sulfur-associated taxa such as members of Desulfovibrionia (Fig. 3, Table S4). Although some taxa differ across studies, similar functional change processes may occur during disease progression, supporting the idea that dysbiosis is functionally consistent but taxonomically variable across regions and host species.

In addition to these statistical trends, this study relied on 16S rRNA gene sequencing, which captures patterns in community composition but does not directly resolve functional roles or pathogenicity. Future research incorporating metagenomic or functional approaches would help clarify the role of specific microbial groups in disease progression.

This study provides one of the few datasets that capture microbial communities before and during SCTLD within the same coral colonies. Overall, the results support a dysbiosis framework in which SCTLD is associated with shifts in microbial communities rather than a single microbial agent.

Declarations

Competing Interests

The author(s) declare that they have no competing interests.

Funding

This work was supported by the National Science Foundation (Award #2000863). Additional support was provided by the Caribbean Regenerative Community Development program through the Puerto Rico Department of Natural and Environmental Resources (PR-DNER; Award #2024-000109-C).

Author Contribution

J.M.G.S. conducted the investigation, performed computational analyses, interpreted the data, prepared figures, and wrote the manuscript. N.V.S., E.W., J.J.C.M., and A.J.V. contributed to study design, field sampling, and manuscript editing. All authors reviewed and approved the final manuscript.

Acknowledgement

We thank the staff and colleagues at the Department of Marine Sciences (UPR-Mayagüez) for assistance with field sampling, laboratory work, and logistic support. We especially acknowledge Yanelle Silva and Guilliana Hernández, who contributed to the initial stages of this project through field sampling and DNA extraction efforts. Additional thanks to all who assisted with sample collection and processing in La Parguera Natural Reserve. We also thank the eDNA Collaborative for supporting participation in the Metabarcoding in Microbial Ecology workshop organized by Physalia Courses.

Data Availability

The raw sequence data generated in this study will be deposited in the NCBI Sequence Read Archive (SRA) and made publicly available upon publication.

References

1. Aeby GS, Ushijima B, Campbell JE, Jones S, Williams GJ, Meyer JL, Hase CC, Paul VJ (2019) Pathogenesis of a tissue loss disease affecting multiple species of corals along the Florida Reef Tract. Front Mar Sci 6:678. https://doi.org/10.3389/fmars.2019.00678
2. Aronson MF, Nilon CH, Lepczyk CA, Parker TS, Warren PS, Cilliers SS, Goddard MA, Hahs AK, Herzog C, Katti M, La Sorte FA, Williams NS, Zipperer W. Hierarchical filters determine community assembly of urban species pools. Ecology. 2016;97(11):2952–2963. DOI: 10.1002/ecy.1535
3. Arriaga-Piñón ZP, Aguayo-Leyva JE, Álvarez-Filip L, Banaszak AT, Aguirre-Macedo ML, Paz-García DA, García-Maldonado JQ (2024) Microbiomes of three coral species in the Mexican Caribbean and their shifts associated with the stony coral tissue loss disease. PLoS One 19:e0304925. https://doi.org/10.1371/journal.pone.0304925
4. Bolyen E, Rideout JR, Dillon MR, Bokulich NA, Abnet CC, Al-Ghalith GA, Alexander H, Alm EJ, Arumugam M, Asnicar F, Bai Y, Bisanz JE, Bittinger K, Brejnrod A, Brislawn CJ, Brown CT, Callahan BJ, Caraballo-Rodríguez AM, Chase J, Cope EK, Da Silva R, Diener C, Dorrestein PC, Douglas GM, Durall DM, Duvallet C, Edwardson CF, Ernst M, Estaki M, Fouquier J, Gauglitz JM, Gibbons SM, Gibson DL, Gonzalez A, Gorlick K, Guo J, Hillmann B, Holmes S, Holste H, Huttenhower C, Huttley GA, Janssen S, Jarmusch AK, Jiang L, Kaehler BD, Kang KB, Keefe CR, Keim P, Kelley ST, Knights D, Koester I, Kosciolek T, Kreps J, Langille MGI, Lee J, Ley R, Liu YX, Loftfield E, Lozupone C, Maher M, Marotz C, Martin BD, McDonald D, McIver LJ, Melnik AV, Metcalf JL, Morgan SC, Morton JT, Naimey AT, Navas-Molina JA, Nothias LF, Orchanian SB, Pearson T, Peoples SL, Petras D, Preuss ML, Pruesse E, Rasmussen LB, Rivers A, Robeson MS II, Rosenthal P, Segata N, Shaffer M, Shiffer A, Sinha R, Song SJ, Spear JR, Swafford AD, Thompson LR, Torres PJ, Trinh P, Tripathi A, Turnbaugh PJ, Ul-Hasan S, van der Hooft JJJ, Vargas F, Vázquez-Baeza Y, Vogtmann E, von Hippel M, Walters W, Wan Y, Wang M, Warren J, Weber KC, Williamson CHD, Willis AD, Xu ZZ, Zaneveld JR, Zhang Y, Zhu Q, Knight R, Caporaso JG (2019) Reproducible, interactive, scalable and extensible microbiome data science using QIIME 2. Nat Biotechnol 37:852–857. https://doi.org/10.1038/s41587-019-0209-9
5. Bourne DG, Morrow KM, Webster NS (2016) Insights into the Coral Microbiome: Underpinning the Health and Resilience of Reef Ecosystems. Annu Rev Microbiol 70:317–40. DOI: 10.1146/annurev-micro-102215-095440
6. Bruno JF, Selig ER, Casey KS, Page CA, Willis BL, et al. (2007) Thermal Stress and Coral Cover as Drivers of Coral Disease Outbreaks. PLOS Biology 5(6): e124. https://doi.org/10.1371/journal.pbio.0050124
7. Burge CA; Eakin CM, Friedman CS, Froelich B, Hershberger PK, Hofmann EF, Petes LE, Prager KC, Weil E, Willis BL, Ford SE and Harvell CW (2014). Climate Change Influences on Marine Infectious

Diseases: Implications for Management and Society. Annu. Rev. Mar. Sci. Vol.6: 249–277. https://doi.org/10.1146/annurev-marine-010213-135029

8. Callahan BJ, McMurdie PJ, Rosen MJ, Han AW, Johnson AJA, Holmes SP (2016) DADA2: high-resolution sample inference from Illumina amplicon data. Nat Methods 13:581–583. https://doi.org/10.1038/nmeth.3869
9. Caporaso JG, Lauber CL, Walters WA, Berg-Lyons D, Huntley J, Fierer N, Owens SM, Betley J, Fraser L, Bauer M, Gormley N, Gilbert JA, Smith G, Knight R (2012) Ultra-high-throughput microbial community analysis on the Illumina HiSeq and MiSeq platforms. ISME J 6:1621–1624. https://doi.org/10.1038/ismej.2012.8
10. Clark AS, Williams SD, Patterson KL, Aeby GS (2021) Characterization of the microbiome of corals with stony coral tissue loss disease along Florida's coral reef. Microorganisms 9:2181. https://doi.org/10.3390/microorganisms9112181
11. Cróquer A, Weil E and Rogers CS (2021) Similarities and Differences Between Two Deadly Caribbean Coral Diseases: White Plague and Stony Coral Tissue Loss Disease. Front. Mar. Sci. 8:709544. https://doi.org/10.3389/fmars.2021.709544
12. Eakin CM, Sweatman HPA, Brainard RE (2019) The 2014–2017 global-scale coral bleaching event: insights and impacts. Coral Reefs 38:1–7. DOI:10.1007/s00338-019-01844-2
13. Ferrario F, Beck MW, Storlazzi CD, Micheli F, Shepard CC, Airoldi L (2014) The effectiveness of coral reefs for coastal hazard risk reduction and adaptation. Nat Commun 5:3794. https://doi.org/10.1038/ncomms4794
14. Harvell, Catherine & Jordán-Dahlgren, Eric & Merkel, Susan & Rosenberg, Eugene & Raymundo, Laurie & Smith, Garriet & Weil, Ernesto & Willis, Bette. (2007). Coral Disease, Environmental Drivers, and the Balance Between Coral and Microbial Associates. Oceanography. 20. https://doi.org/10.5670/oceanog.2007.91
15. Harvell, C. D., Montecino-Latorre, D., Caldwell, J. M., Burt, J. M., Bosley, K., Keller, A., Heron, S. F., Salomon, A. K., Lee, L., Pontier, O., Pattengill-Semmens, C., & Gaydos, J. K. (2019). Disease epidemic and a marine heat wave are associated with the continental-scale collapse of a pivotal predator (Pycnopodia helianthoides). Science Advances, 5(1), eaau7042. https://doi.org/10.1126/sciadv.aau7042
16. Hernández-Delgado EA (2015) The emerging threats of climate change on tropical coastal ecosystem services, public health, local economies and livelihood sustainability of small islands: cumulative impacts and synergies. Mar Pollut Bull 101:5–28. https://doi.org/10.1016/j.marpolbul.2015.09.018
17. Hoegh-Guldberg, Ove & Mumby, Peter & Hooten, A.J. & Steneck, R.S. & Greenfield, Paul& Gomez, Erick & Harvell, Catherine & Sale, Peter & Edwards, Alasdair & Caldeira,Ken & Knowlton, Nancy & Eakin, C. Mark & Iglesias-Prieto, Roberto & Muthiga, Nyawira& Bradbury, Roger & Dubi, Alfonse & Hatziolos, M. (2008). Coral Reefs Under Rapid Climate Change and Ocean Acidification. Science (New York, N.Y.). 318. 1737-42. DOI:10.1126/science.1152509

18. Hughes, T.P. (1994) Catastrophes, Phase Shifts, and Large-Scale Degradation of a Caribbean Coral Reef. Science, 265, 1547–1551. http://dx.doi.org/10.1126/science.265.5178.1547
19. Hughes, Terence & Baird, Andrew & Bellwood, David & Card, Margaret & Connolly, Sean& Folke, Carl & Grosberg, Richard & Hoegh-Guldberg, Ove & Jackson, JBC & Kleypas,Janice. (2003). Climate change, human impacts, and the resilience of coral reefs.science. 301. 929–933.
20. Hughes TP, Kerry JT, Álvarez-Noriega M, Álvarez-Romero JG, Anderson KD, Baird AH, Babcock RC, Beger M, Bellwood DR, Berkelmans R, Bridge TCL, Butler IR, Byrne M, Cantin NE, Comeau S, Connolly SR, Cumming GS, Dalton SJ, Diaz-Pulido G, Eakin CM, Figueira WF, Gilmour JP, Harrison HB, Heron SF, Hoey AS, Hobbs JPA, Hoogenboom MO, Kennedy EV, Kuo CY, Lough JM, Lowe RJ, Liu G, McCulloch MT, Malcolm HA, McWilliam MJ, Pandolfi JM, Pears RJ, Pratchett MS, Schoepf V, Simpson T, Skirving WJ, Sommer B, Torda G, Wachenfeld DR, Willis BL, Wilson SK (2017) Global warming and recurrent mass bleaching of corals. Nature 543:373–377. https://doi.org/10.1038/nature21707
21. Huntley N, Brandt ME, Becker CC, Miller CA, Meiling SS, Correa AMS, Holstein DM, Muller EM, Mydlarz LD, Smith TB, Apprill A (2022) Experimental transmission of stony coral tissue loss disease results in differential microbial responses within coral mucus and tissue. ISME Communications 2:46. https://doi.org/10.1038/s43705-022-00126-3
22. Jackson JBC, Donovan MK, Cramer KL, Lam VY, Bak RM, Chollett I, Connolly SR, Cortés J, Dustan P, Eakin CM, Friedlander AM, Greenstein BJ, Heron S, Hughes T, Miller J, Mumby P, Pandolfi JM, Rogers CS, Steneck S, Weil E (+ 58 authors) (2014). Status and Trends of Caribbean Coral Reefs: 1970–2012. Global Coral Reef Monitoring Network, IUCN, Gland, Switzerland. 304 pp
23. Jari Oksanen, Blanchet, F. G., Friendly, M., Kindt, R., Legendre, P., McGlinn, D., Minchin, P. R., O'Hara, R. B., Simpson, G. L., Solymos, P., Stevens, M. H. H., Szoecs, E., & Wagner, H. (2022). vegan: Community Ecology Package. R package version 2.6-4. 10.32614/CRAN.package.vegan
24. Knowlton N, Rohwer F (2003) Multispecies microbial mutualisms on coral reefs: the host as a habitat. Am Nat 162:S51-S62. https://doi.org/10.1086/378684
25. Landsberg JH, Kiryu Y, Peters EC, Wilson PW, Perry N, Waters Y, Voss JD, Nuttle D, Voss E, Patterson KL (2020) Stony coral tissue loss disease in Florida is associated with disruption of host-zooxanthellae physiology. Front Mar Sci 7:576. https://doi.org/10.3389/fmars.2020.576013
26. Lucas MQ, Collazo Roman DL, Mercado MA, et al. (2024) Stony coral tissue loss disease (SCTLD) induced mass mortality at Arecibo, Puerto Rico. Mar Biodivers 54:10. https://doi.org/10.1007/s12526-023-01393-6
27. McClanahan, T. R., & Muthiga, N. A. (2017). Environmental variability indicates a climate-adaptive center under threat in northern Mozambique coral reefs. Ecosphere, 8(5), e01812. https://doi.org/10.1002/ecs2.1812
28. McClanahan T, Weil E, Baird A (2018). Impact of Bleaching on Coral Reefs. In Van Oppen M (Edit). Coral Bleaching (second edition). Springer. Pp.231–264.

29. Meyer JL, Castellanos-Gell J, Aeby GS, Häse CC, Ushijima B, Paul VJ (2019) Microbial community shifts associated with the ongoing of stony coral tissue loss disease outbreak on the Florida Reef Tract. Front Microbiol 10:2249. DOI: 10.3389/fmicb.2019.02244
30. Moberg F, Folke C (1999) Ecological goods and services of coral reef ecosystems. Ecol Econ 29:215–233. https://doi.org/10.1016/S0921-8009(99)00009-9
31. Nandi S, Stephens TG, Walsh K, García-Camps R, Villalpando MF, Sellares-Blasco RI, Zubillaga AL, Croquer A, Bhattacharya D (2025) Shifts in the microbiome and virome are associated with stony coral tissue loss disease. ISME Commun 5. https://doi.org/10.1093/ismeco/ycaf226
32. Peixoto RS, Rosado PM, Leite DCDA, Rosado AS, Bourne DG (2017) Beneficial microorganisms for corals (BMC): proposed mechanisms for coral health and resilience. Front Microbiol 8:341. https://doi.org/10.3389/fmicb.2017.00341
33. Precht WF, Gintert BE, Robbart ML, Fura R, van Woesik R (2016) Unprecedented disease-related coral mortality in southeastern Florida. Sci Rep 6:31374. https://doi.org/10.1038/srep31374
34. Reaka-Kudla ML (1997) The global biodiversity of coral reefs: a comparison with rain forests. In: Reaka-Kudla ML, Wilson DE, Wilson EO (eds) Biodiversity II: understanding and protecting our biological resources. Joseph Henry Press, pp 83–108
35. Rogers CS (1993) Hurricanes and coral reefs: the intermediate disturbance hypothesis revisited. Coral Reefs 12:127–137. https://doi.org/10.1007/BF00334471
36. Rosenberg E, Koren O, Reshef L, Efrony R, Zilber-Rosenberg I (2007) The role of microorganisms in coral health, disease and evolution. Nat Rev Microbiol 5:355–362. https://doi.org/10.1038/nrmicro1635
37. Rosales SM, Miller MW, Williams DE, Traylor-Knowles N (2023) Rhodobacterales and Rhizobiales Are Associated With Stony Coral Tissue Loss Disease and Its Suspected Sources of Transmission. Front Microbiol 11:681. https://doi.org/10.3389/fmicb.2020.00681
38. Rossin, A.M., Beavers, K.M., Karrick, C.E. et al. Runaway coral-algal dysbiosis may be responsible for rapid coral tissue loss. Sci Rep 16, 6415 (2026). https://doi.org/10.1038/s41598-026-35666-4
39. Ushijima B, Meyer JL, Thompson S, Pitts K, Marusich MF, Tittl J, Weatherup E, Reu J, Wetzell R, Aeby GS, Häse CC, Paul VJ (2020) Disease Diagnostics and Potential Coinfections by Vibrio coralliilyticus During an Ongoing Coral Disease Outbreak in Florida. Sci Rep 10:19610. https://doi.org/10.3389/fmicb.2020.569354
40. van Oppen MJH, Blackall LL (2019) Coral microbiome dynamics, functions and design in a changing world. Nat Rev Microbiol 17:557–567. https://doi.org/10.1038/s41579-019-0223-4
41. Vega Thurber R, Mydlarz L, Brandt M, Harvell D, Weil E, Raymundo L, Willis BL, Langevin S, Tracy AM, Littman R, Kemp KM, Dawkins P, Prager KC, Garren M and Lamb J. 2020. Deciphering Coral Disease Dynamics: Integrating Host, Microbiome, and the Changing Environment. Front. Ecol. Evol. 8:575927. https://doi.org/10.3389/fevo.2020.575927
42. Weil E, Croquer A and Urreiztieta I (2009a). Temporal variability and consequences of coral diseases and bleaching in La Parguera, Puerto Rico from 2003–2007. Carib. J Sci Vol 45, N˚ 2–3:221–246.

43. Weil E, Cróquer A and Urreiztieta I (2009b). Yellow band disease compromises the reproductive
44. output of the reef-building coral Montastraea faveolata (Anthozoa, Scleractinia). Dis Aquat Organ. 2009;87(1–2):45–55. doi: 10.3354/dao02103
45. Rogers, C.S., and Weil, E., 2010, Coral reef diseases in the Atlantic-Caribbean, chap. of Coral reefs: An ecosystem in transition, p. 465–492, https://doi.org/10.1007/978-94-007-0114-4_27.
46. Weil, E., Rogers, C.S., Croquer, A. (2017). Octocoral Diseases in a Changing Ocean. In: Rossi, S., Bramanti, L., Gori, A., Orejas, C. (eds) Marine Animal Forests. Springer, Cham. https://doi.org/10.1007/978-3-319-21012-4_43
47. Weil E, Hernández-Delgado EA, Gonzalez M, Williams S, Suleimán-Ramos S, Figuerola M, Metz-Estrella T (2019). Spread of the New Coral Disease “SCTLD” into the Caribbean: Implications for Puerto Rico. Reef Encounters. Vol. 34 (1):38–43.
48. Williams SM, García-Sais J, Sabater-Clavell J (2021) Prevalence of stony coral tissue loss disease at El Seco, a mesophotic reef system off Vieques Island, Puerto Rico. Front Mar Sci 8:668669. https://doi.org/10.3389/fmars.2021.668669
49. Zaneveld JR, McMinds R, Vega Thurber R (2016) Overfishing and nutrient pollution interact with temperature to disrupt coral reefs. Nat Commun 7:11833. https://doi.org/10.1038/ncomms11833

Figures

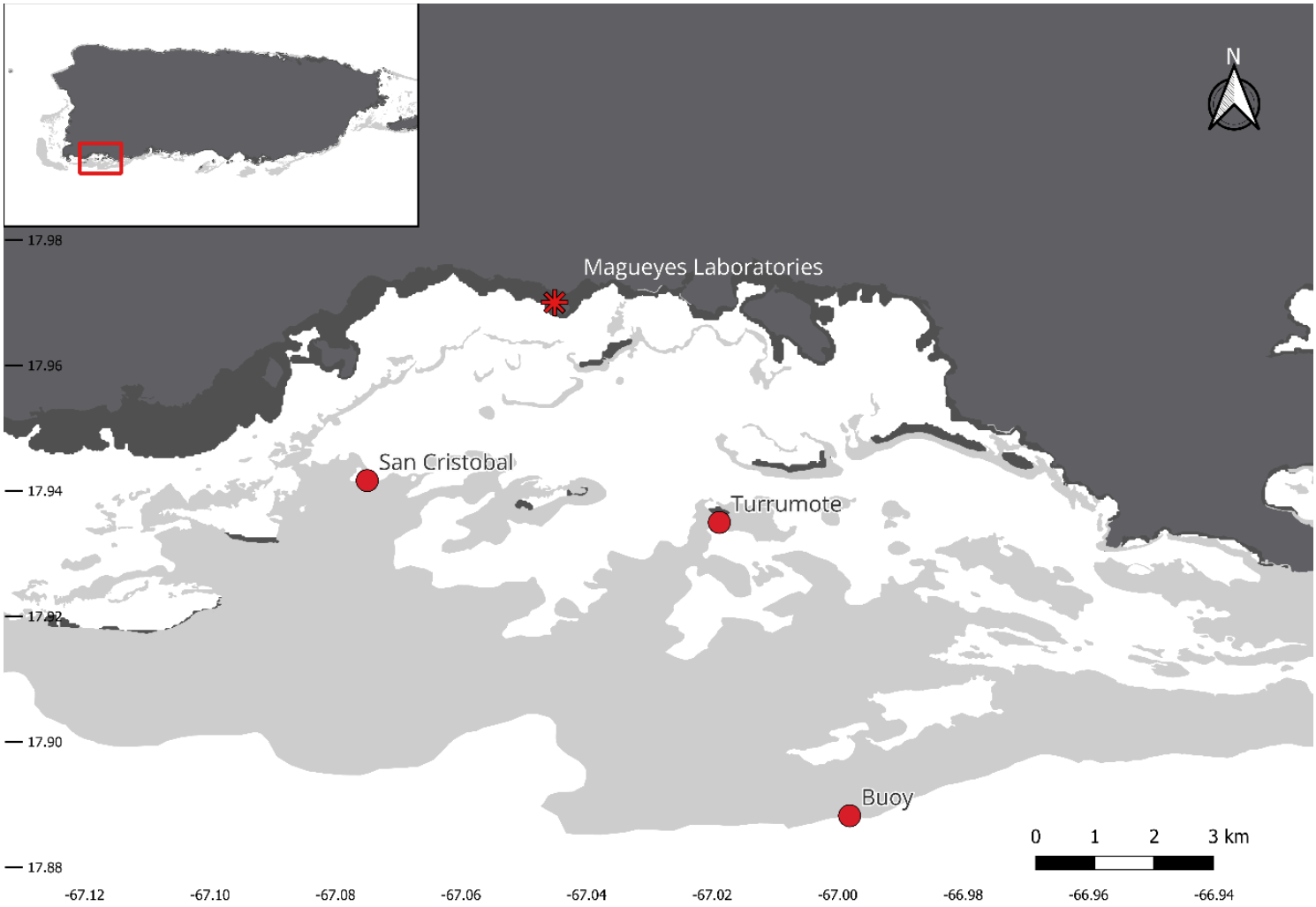


Figure 1

Map of the study area in the La Parguera Natural Reserve (LPNR), southwestern Puerto Rico, showing the sampling sites included in this study: San Cristóbal, Turrumote, and Buoy. The location of LPNR within Puerto Rico is indicated in the inset (red box). Samples were collected from multiple scleractinian coral species across these sites as part of long-term monitoring efforts before and after the onset of Stony Coral Tissue Loss Disease (SCTLD). The location of the Department of Marine Sciences at Isla Magueyes is also shown.

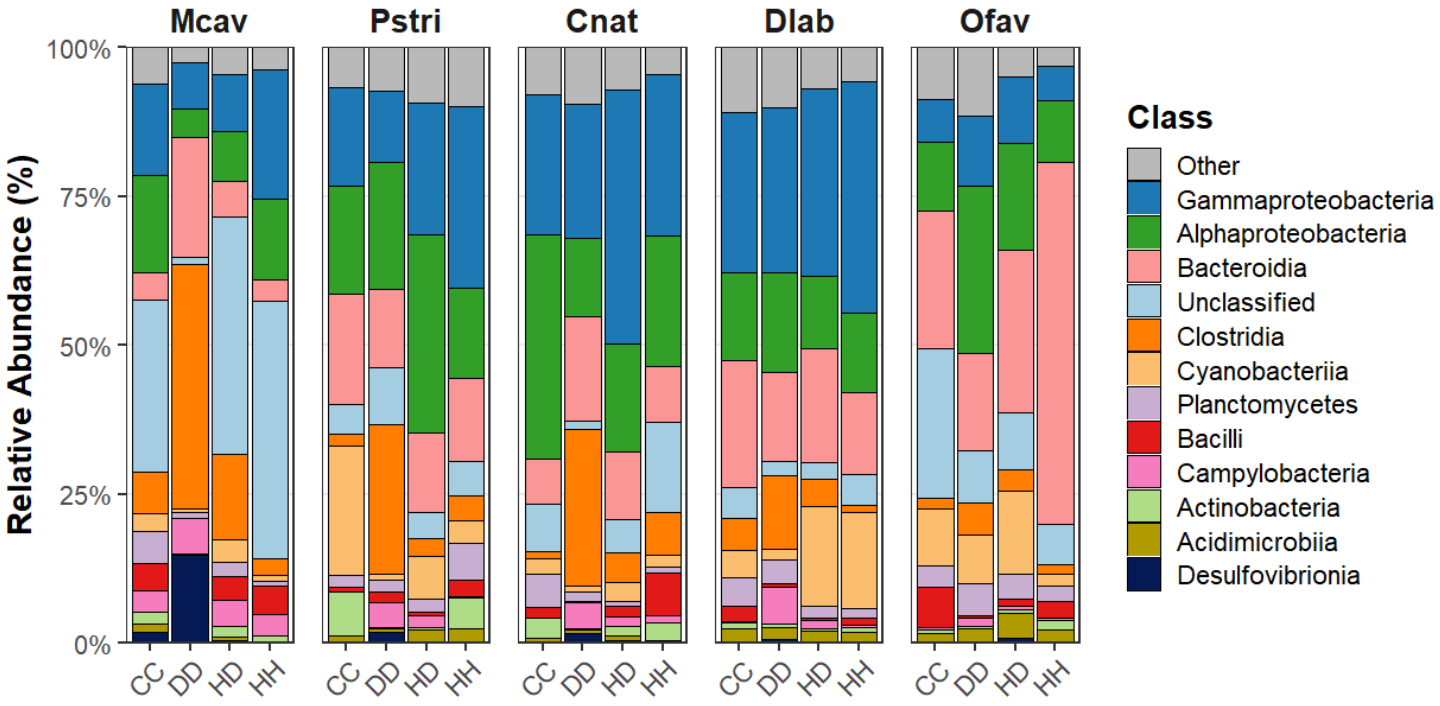


Figure 2

Relative abundance of dominant bacterial taxa across five coral species and health states. Taxa are shown at the class level and represent the most abundant groups across all samples. Each bar corresponds to a health state for each species: healthy colonies (HH), diseased lesion tissue (DD), apparently healthy tissue from diseased colonies (HD), and control colonies without visible lesions (CC).

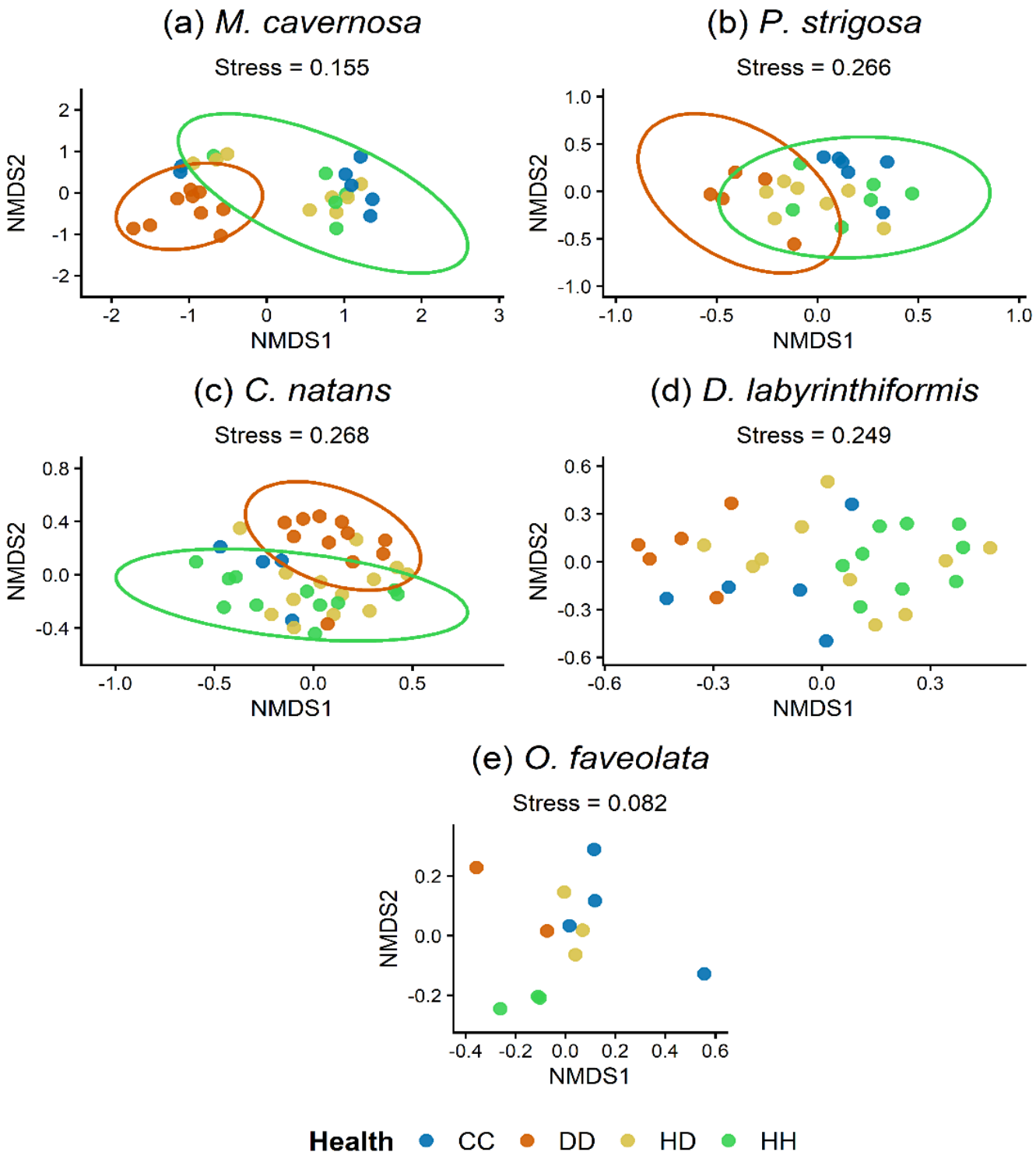


Figure 3

Non-metric multidimensional scaling (NMDS) ordination of microbial community composition based on Bray-Curtis dissimilarity. Each point represents a sample, colored by health state. Samples are grouped by coral species, and ellipses indicate clustering of selected groups (e.g., HH and DD). Stress values are shown for each ordination. Differences in community composition were tested using PERMANOVA. Health conditions are defined as follows: HH = apparently healthy colonies sampled prior to SCTLD

detection in La Parguera Natural Reserve; DD = lesion margin tissue from diseased colonies; HD = apparently healthy tissue within diseased colonies; CC = visually healthy control colonies sampled at the same time and sites as diseased colonies.



Figure 4

Heatmap showing differentially abundant bacterial genera across health states (CC, HH, HD, DD) in five coral species. Taxa are displayed at the genus level and grouped by species. Color intensity represents log10-transformed relative abundance, with darker colors indicating higher values. Asterisks indicate statistically significant differences between health states (**p < 0.01, ***p < 0.001). Only taxa meeting thresholds are shown, and taxa are ordered within each species based on mean abundance in diseased samples

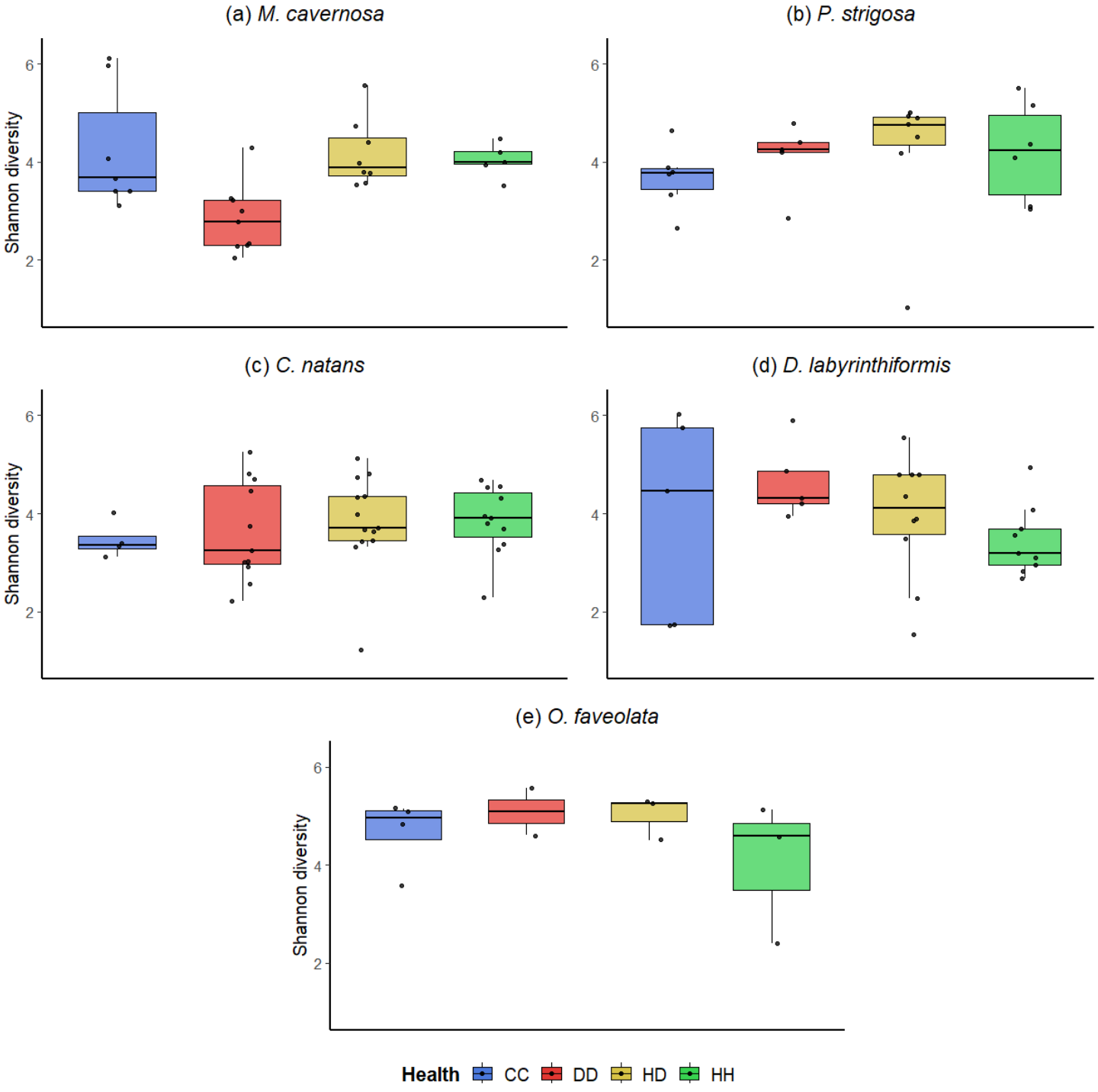


Figure 5

Alpha diversity of coral-associated bacterial communities across species and health states, measured using the Shannon diversity index. Health states include apparently healthy colonies (**HH**), lesion margin samples from diseased colonies (**DD**), apparently healthy tissue within diseased colonies (**HD**), and nearby unaffected control colonies (**CC**). Each point represents an individual sample, and boxplots summarize distributions within each group. Statistical differences among groups were assessed using non-parametric tests.

Supplementary Files

This is a list of supplementary files associated with this preprint. Click to download.

- TableS1ShannonKruskal.csv
- TableS2ShannonWilcoxon.csv
- TableS3PERMANOVA.csv
- TableS4DifferentialabundanceKruskal.csv